SIMULATION OF A LINEAR PIEZOELECTRIC MOTOR BY USING FINITE ELEMENT METHOD

Humberto Ferreira Vinhais
Escola Politécnica da Universidade de São Paulo
Av. Prof. Mello de Moraes, 2231, São Paulo –SP – 05508-900
humberto.vinhais@poli.usp.br

Ricardo Cury Ibrahim
Escola Politécnica da Universidade de São Paulo
Av. Prof. Mello de Moraes, 2231, São Paulo –SP – 05508-900

Emilio Carlos Nelli Silva
Escola Politécnica da Universidade de São Paulo
Av. Prof. Mello de Moraes, 2231, São Paulo –SP – 05508-900

Abstract. *Piezoelectric materials convert electrical energy into mechanical energy. These materials are widely used for building devices such as sensors, actuators, piezoelectric motors, ultrasonic transducers, etc. A linear piezoelectric motor is considered in this study. It consists of two piezoceramics at 90 degrees connected to an aluminum structure with a complex geometry. The structure vibration generates an elliptical movement at surface points that moves by friction a thin metal bar in the horizontal direction. Due to the complexity of the coupling structure, analytical models cannot be applied to model it. Therefore, in this work, the motor behavior was analyzed by using Finite Element Method (FEM) through ANSYS software. The simulation takes into account piezoelectric effect, structural damping and its electrical driving circuit. Harmonic and transient analyses were conducted which allowed us to obtain a simulation of the mechanical and electrical motor behavior taking into account its electrical driving circuit. Based on these simulation results, it was possible to better understand motor behavior and thus to calculate its optimum excitation frequency, to obtain a better performance. The developed simulation methodology and modeling can be applied to other types of linear piezoelectric motors.*

Keywords*: piezoelectric motor, ultrasonic motor, finite element method, piezoelectric circuit simulation, computational simulation*

1. Introduction

The piezoelectric materials can contract and expand in accordance to the applied electrical voltage to its terminals and vice versa. Furthermore, the piezoelectric materials are generally used in accelerometers, pressure and force sensors, ultrasonic transducers, nanoactuators and other devices. Nowadays, its application as ultrasonic motor or actuators in high precision mechanics is growing rapidly.

A piezoelectric motor consists of two or more piezoelectric ceramic connected to a metallic structure (generally aluminum because of its high flexibility) with specific forms and configurations. These piezoceramics are excited with alternated electrical voltages with different phases, which generate the vibration of the structure, called stator (see Fig. (1)). The movement of vibration of the metallic structure results in the propagation of a mechanical wave which creates an elliptical movement in the point of contact of the stator with a thin metal bar, called carriage (see Fig. (1)), which moves by friction in the horizontal direction (Sashida, 1993). The approach of how to get this elliptical movement in the contact point mainly depend on the form and disposal of piezoceramics and the geometry of the flexible structure which defines the type of piezoelectric motor. There are two types of piezoelectric motors: rotational and linear. A linear piezoelectric motor is studied in this work.

The use of the Finite Element Method (FEM) to model these motors has already been proposed by many works (Kagawa, 1996). Rotational piezoelectric motors are recently used in production lines to control high precision devices (Kagawa, 1996; Sashida, 1993). Linear piezoelectric motors have a wide application in nanometric precision actuators, as quasi-static piezoelectric motors (low operational frequency), or as ultrasonic piezoelectric motors. Quasi-static piezoelectric motors are widely applied as inchworm motors for micro-positioning systems (Frank, 1999; Roberts, 1999). Ultrasonic linear piezoelectric motors have been widely applied to control the precision of many engineering devices, such as tool devices for numerical control lathes (CNC) (Kurosawa, 1998).

The objective of this work is the development of a methodology for simulation of linear piezoelectric motors using software ANSYS, to obtain the mechanical stresses behavior of piezoelectric motor in movement, analyze its ellipses of movement, find an optimum operational frequency and perform a simulation of piezoelectric motors with its electrical driving circuits. For the visualization of the mechanical stresses and for the calculation of the ellipses of movement of the motor, it was necessary to interact with the commercial software MATLAB.

The motor studied in this project consists essentially of two piezoelectric ceramics disposed in 90 degrees, an aluminum stator connected to the piezoceramics and the carriage, which moves horizontally by friction. This motor operates in ultrasonic frequencies (42 kHz).

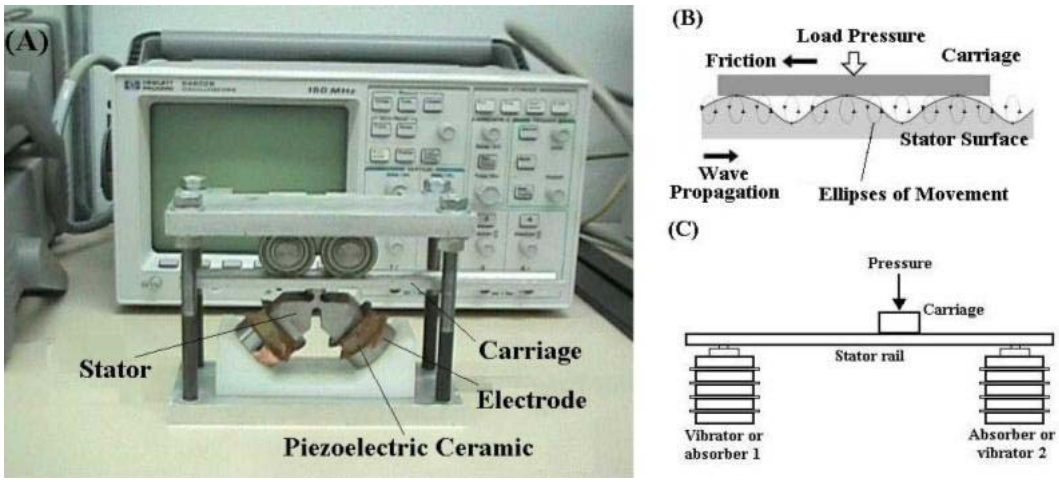

Figure 1. (A) Motor in study; (B) Movement of the stator tip; (C) the Langevin motor

This article is organized as follows: in section 2, the principles of the linear piezoelectric motors are presented. In section 3, the main equations of the piezoelectric FEM, with a theoretical presentation of the circuit analysis, are described. Section 4 presents a developed methodology for simulating the motor using ANSYS. In section 5, the main results and its conclusions are presented. In section 6, the results acquired from simulations are summarized and future works are described.

2. Principles of piezoelectric motors

The piezoelectric ceramic vibration generates a specific wave movement in the motor structure (in the stator) which, by friction, moves a second structure (rotor or the carriage, for linear movements), characterizing the piezoelectric motor. Generally, the ceramics are excited with alternated voltage, thus generating alternated movements. The composition of these movements results in a harmonic movement.

This wave movement generates an ellipse due to the composition of the displacements of two ceramics, as it can be seen in Fig. (1) (Sashida, 1993).The formation of this ellipse in the tip of the stator together with a load pressure applied to the structure in contact (the carriage or the rotor) causes the movement of the same stator, which can be noted in Fig. (1b):

The velocity in the highest point of the ellipse determines the speed of the contact point between the stator and the carriage, which means, the speed of the carriage itself. The ellipse of movement allows us to calculate the speed of the carriage, being a crucial point for the motor movement analysis.

Before continuing, the operation of the Langevin motor, presented in the Fig. (1), must be better understood, once this motor represents a generic linear piezoelectric motor. It can be noticed that one stack of piezoceramics is the vibrator and the other one is the absorber. If only one stack of piezoceramics is considered as the vibrator, the traveling mechanical wave would reflect at the end of the beam (stator rail) and would return creating destructive interferences. Thus, it would not be possible to move the carriage (to see figure above), once a stationary wave is created. Thus, two stacks of piezoelectric ceramics are placed, to eliminate (to absorb) this traveling wave before arriving at the end of the beam, preventing that the wave be reflected (Sashida, 1993).

To understand the principle of the motor design, Eq. (1) is considered. First, the velocity (v) described in this equation depends on the material and on the motor structure geometry in which the wave propagates. Therefore, the velocity is a fixed value for the motor. However, the frequency (f) and the wavelength (λ) can vary.

$$v = \lambda . f \tag{1}$$

Essentially, to design a piezoelectric motor, the operational frequency is fixed and the expected value of the wavelength is calculated (see Eq. (1)). Thus, the absorber is placed in a specific distance to the vibrator which is a multiple of the wavelength. In the case that this distance is fixed (which happens with the studied motor), it is necessary to find the wave frequency whose value of wavelength has this distance as a multiple. While this wavelength is not found, theoretically, a part of the wave would not be absorbed, would reflect and destructively interfere with its own signal. Thus, when the frequency is changed, the size of the ellipse of movement changes too. This means that the frequency which generates the largest ellipse of movement gives us the wavelength that optimizes the system. This frequency is called optimum operational frequency.

3. Piezoelectric FEM

To model the motor of Fig. (1), through FEM (Finite Element Method), ANSYS software is used. FEM equilibrium equations for piezoelectric medium are briefly described.

Piezoelectric FEM equations can be written in terms of nodal displacement {U} and nodal electrical potential {Φ} for each node. The mechanical efforts are expressed by {F} and the nodal electric loads, by {Q}, resulting in the equilibrium equations below (Lerch, 1990; Ostergaard, 1986).

$$[M_{uu}]\{\ddot{U}\}+[C_{uu}]\{\dot{U}\}+[K_{uu}]\{U\}+[K_{u\phi}]\{\phi\}=\{F\} \tag{2}$$

$$[K_{u\phi}]^T\{U\}+[K_{\phi\phi}]\{\phi\}=\{Q\} \tag{3}$$

This same expression can also be expressed in the matrical form:

$$\begin{bmatrix}[M_{uu}] & 0\\ 0 & 0\end{bmatrix}\begin{Bmatrix}\{\ddot{U}\}\\ \{\ddot{\phi}\}\end{Bmatrix}+\begin{bmatrix}[C_{uu}] & 0\\ 0 & 0\end{bmatrix}\begin{Bmatrix}\{\dot{U}\}\\ \{\dot{\phi}\}\end{Bmatrix}+\begin{bmatrix}[K_{uu}] & [K_{u\phi}]\\ [K_{u\phi}]^T & [K_{\phi\phi}]\end{bmatrix}\begin{Bmatrix}\{U\}\\ \{\phi\}\end{Bmatrix}=\begin{Bmatrix}\{F\}\\ \{Q\}\end{Bmatrix} \tag{4}$$

where:

$$[K_{uu}]=\iiint_{\Omega e}[B_u]^T[c][B_u]dV\ ;\ [K_{u\phi}]=\iiint_{\Omega e}[B_u]^T[e][B_\phi]dV\ ;\ [K_{\phi\phi}]=\iiint_{\Omega e}[B_\phi]^T[\varepsilon][B_\phi]dV\ ;\ [M_{uu}]=\rho\iiint_{\Omega e}[N_u]^T[N_u]dV\ ;$$
$$[C_{uu}]=\beta[K_{uu}] \tag{5}$$

where: $[K_{uu}]$ – mechanical stiffness matrix.
$[K_{u\Phi}]$ – piezoelectric coupling matrix.
$[K_{\Phi\Phi}]$ – dielectric stiffness matrix.
$[M_{uu}]$ – mass matrix.
$[C_{uu}]$ – mechanical damping matrix.
$[B_u]$, $[B_\Phi]$- derivatives of FEM shape functions
[c] – elastic coefficients
[e] – piezoelectric coefficients
[ε] – dielectric coefficients
β – damping coefficient.

3.1. Harmonic Analysis

In the simulation of the piezoelectric motor studied, the piezoceramics are excited with sinusoidal (harmonic) electrical voltage. The harmonic analysis allows the observation of the piezoelectric structure under the influence of harmonic forces, displacements, electrical charges or electrical potentials (as it is the case of the motor studied).

In this case, forces, displacements, electrical charges and electrical potential, respectively, are expressed by the following form:

$$\{F(t)\}=\{F\}e^{j.\omega.t}\ ;\ \{U(t)\}=\{U\}e^{j.\omega.t}\ ;\ \{Q(t)\}=\{Q\}e^{j.\omega.t}\ ;\ \{\phi(t)\}=\{\phi\}e^{j.\omega.t} \tag{6}$$

where ω is the exciting frequency.

It is worth to remember that these values of {U},{Φ}, {F}, {Q} present real numbers, when the system does not have damping, and complex numbers when there is damping, which means the addition of a phase displacement.

Substituting Eq. (6) in the piezoelectric constitutive Eqs. (2) and (3), it can be written as:

$$\begin{bmatrix}K_{uu}+j.\omega.C_{uu}-\omega^2.M_{uu} & K_{u\phi}\\ K_{u\phi}{}^T & K_{\phi\phi}\end{bmatrix}\begin{Bmatrix}\hat{U}\\ \hat{\phi}\end{Bmatrix}=\begin{Bmatrix}\hat{F}\\ \dfrac{1}{j.\omega}.\hat{I}\end{Bmatrix} \tag{7}$$

where ^ represents complex matrices.

Harmonic analysis allows us determining the frequency response of the piezoelectric structure's characteristics (Lerch, 1990; Moaveni, 1999; Ostergaard, 1986).

It is worthy to emphasize that, in a harmonic analysis, ANSYS only supplies the real and imaginary values of the mechanical stresses and the displacements in X and in Y directions. Therefore, to obtain its amplitude values, it is necessary to calculate it (what can be done in MATLAB). Thus, initially, the amplitude value for each element (or node) of the structure is calculated and, to obtain the desired value at any time, the amplitude vector must be rotated in 360°.

3.2. Transient Analysis

In transient analysis, Eqs. (2) and (3) are solved considering F(t) and Q(t) as generic functions of time. These functions are defined, specifying the value of the function for different increments of time. The function is divided in load steps, each one contains one or more increments of time (Lerch, 1990; Ostergaard, 1986).

For the solution of the transient problem, ANSYS uses an implicit method of integration (Newmark), where Eqs. (2) and (3) are solved in a period of time (Lerch, 1990; Ostergaard, 1986). Essentially, $[M_{uu}]\{\ddot{U}\}$ e $[C_{uu}]\{\dot{U}\}$ are interpreted as forces of inertia and viscosity, respectively, and the static equilibrium in each instant of time is imposed.

3.3. Circuit Analysis

For the simulation of piezoelectric motors together with its electrical driving circuits, harmonic and transient analysis were performed to solve electrical circuits equations. For this type of analysis, ANSYS defines a circuit element: CIRCU94. This element is recommended for piezoelectric circuit analysis, once it presents a more appropriate formulation for the simulations of piezoceramics with electrical circuits. The harmonic analysis must be used for obtaining frequency response with the use of a source of constant electrical voltage amplitude (Wang, 1999). The transient analysis must be used for many types of source of electrical voltage that can change with time, as sources allowing the generation of sinusoidal, square shaped and triangular waves for electrical voltage.

In circuit transient analysis, ANSYS uses the Trapezoidal Method for the step (n+1) (Wang, 1999), generating the following equations to define the capacitor and the resistor behavior, respectively.

$$\begin{bmatrix} C & -C \\ -C & C \end{bmatrix}\begin{Bmatrix} V_1 \\ V_2 \end{Bmatrix} = \begin{Bmatrix} -Q_C{}^{n+1} \\ Q_C{}^{n+1} \end{Bmatrix} \; ; \; \left(\frac{\theta\Delta t}{R}\right)\begin{bmatrix} 1 & -1 \\ -1 & 1 \end{bmatrix}\begin{Bmatrix} V_1{}^{n+1} \\ V_2{}^{n+1} \end{Bmatrix} = -\begin{Bmatrix} -Q_{RS} \\ Q_{RS} \end{Bmatrix} \tag{8}$$

In harmonic analysis, the capacitor and the resistor have the following equations:

$$\begin{bmatrix} C & -C \\ -C & C \end{bmatrix}\begin{Bmatrix} V_1 \\ V_2 \end{Bmatrix} = \begin{Bmatrix} 0 \\ 0 \end{Bmatrix} \; ; \; j\omega\left(-\frac{1}{\omega^2.R}\right)\begin{bmatrix} 1 & -1 \\ -1 & 1 \end{bmatrix}\begin{Bmatrix} V_1 \\ V_2 \end{Bmatrix} = \begin{Bmatrix} 0 \\ 0 \end{Bmatrix} \tag{9}$$

4. Motor computational simulation

Figure (1) describes the motor finite element model constructed in ANSYS. The information about material properties, for the computational simulation, is presented in the Appendix A. As already mentioned, the motor in study must be excited with a sign wave of electrical voltage of 500V amplitude and 42 kHz of central frequency, 90° phase difference of between the exciting signals of each piezoelectric ceramic (same of experiments).

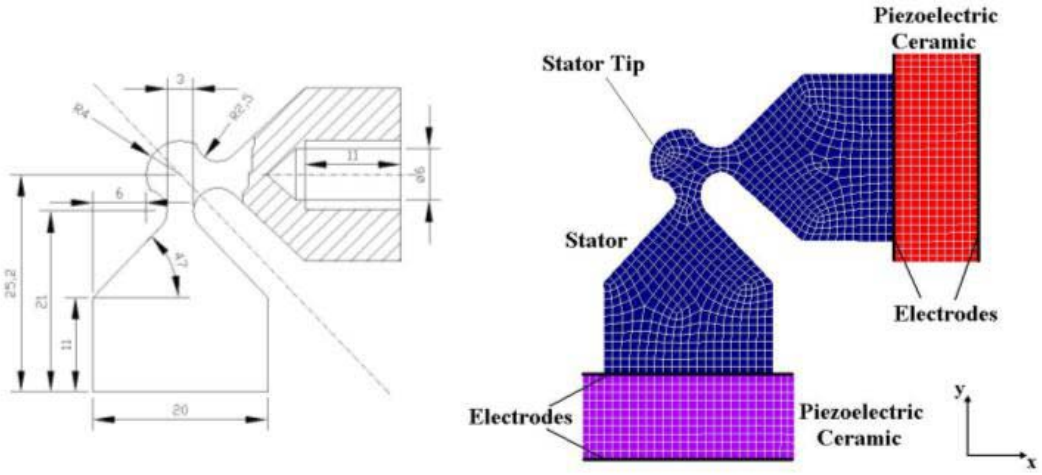

Figure 2. FEM 2D model of the motor in study (to the right) and its design dimensions (to the left).

The FEM model of the motor in study is presented in the figure above. For this motor, a bidimensional model was built because of the structure prismatic shape. This FEM model contains 1286 finite elements and 1402 nodes. Another important aspect for the motor simulation is the boundary conditions. In this case, the displacement in X and in Y directions at the

base of each ceramic was restrained, therefore, as it can be seen in Fig. (1), this is the region where the motor is fixed. For FEM modeling in ANSYS, the element of type PLANE42 and PLANE13 had been used (both considered Plane Stress), together with the properties of each material (Appendix A).

To obtain ellipses of movement and velocity, a routine of MATLAB was created. For this routine, output data from a harmonic analysis in ANSYS (real and imaginary values) is used as input data.

To calculate the velocity, the displacement of each axis can be written using following expressions:

$$X = u_x.\cos(\omega.t + \varphi_x) \; ; Y = u_y.\cos(\omega.t + \varphi_y) \tag{10}$$

where: X e Y are the displacements in x and y directions, respectively.
u_x e u_y are the amplitudes of these displacements in x and y directions, respectively.
φ_x e φ_y are the phases of each axis.

Derivating Eq. (10), the values of the velocities, V_x and V_y , can be found:

$$V_x = u_x.\omega.sen(\omega.t + \varphi_x); \; V_y = u_y.\omega.sen(\omega.t + \varphi_y) \tag{11}$$

Thus, Eq. (11) can be written in absolute values, as the modulus of velocity V:

$$V = \sqrt{{V_x}^2 + {V_y}^2} \tag{12}$$

Thus, the modulus of the velocity can be obtained applying Eq. (12) for each point of the ellipse and its direction is simply tangent to the ellipse at the point in study.

As already mentioned, the harmonic analysis supplies the results as real and imaginary values, however these values are not given by ANSYS for each instant of time in the operation of the motor. For this reason, the structure was rebuilt in a MATLAB routine for each instant of time. The output data of this routine was returned to ANSYS as an input data. Thus it was possible to capture images from ANSYS for each instant of time and to create an animation (as it will be shown ahead).

In Appendix B, the frequency spectrum of the applied electrical voltage signal is presented by considering the same simulation through a transient analysis. However, the frequency spectrum shows some undesirable frequencies, which justifies the use of a harmonic analysis for this simulation.

For the simulation of the motor together with its electrical driving circuit, a FEM model of the circuit was built as shown in the figure below.

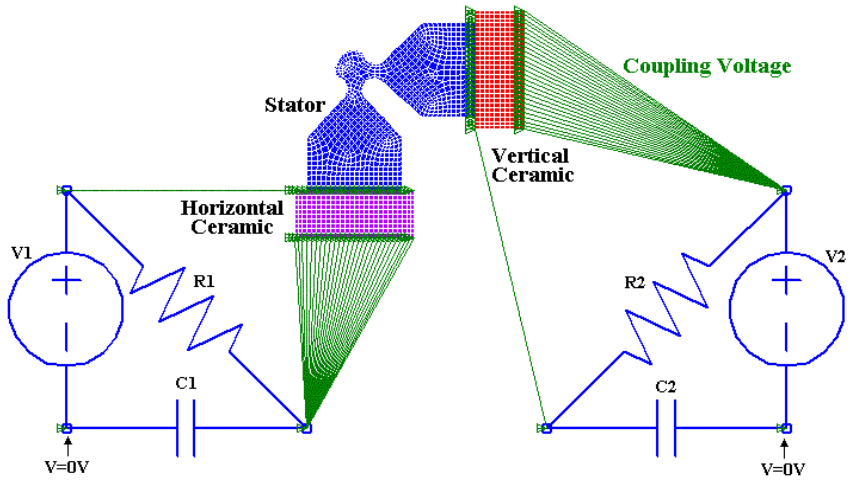

Figure 3. The piezoelectric motor in study together with is electrical driving circuit.

In the circuit above, the node indicated with V=0V have null electrical potential (grounded), R1=R2=200, C1=C2=100μF and V1=V2 indicates an electrical source of 500V with 42 kHz. The electrical voltage signal of the source V2 has a phase of 90° in relation to the signal of V1. The circuit above is simulated in transient analysis, as it was already commented.

5. Results

5.1. Ellipses of Movement

From the presented theoretical development, the ellipses of movement of the motor are obtained through a harmonic analysis in ANSYS. In the figure bellow, the ellipses of movement of the motor in study for two distinct cases are represented: within and without damping. These graphs were obtained considering the treatment of ANSYS results using MATLAB, by using Eqs. (10) to (12).

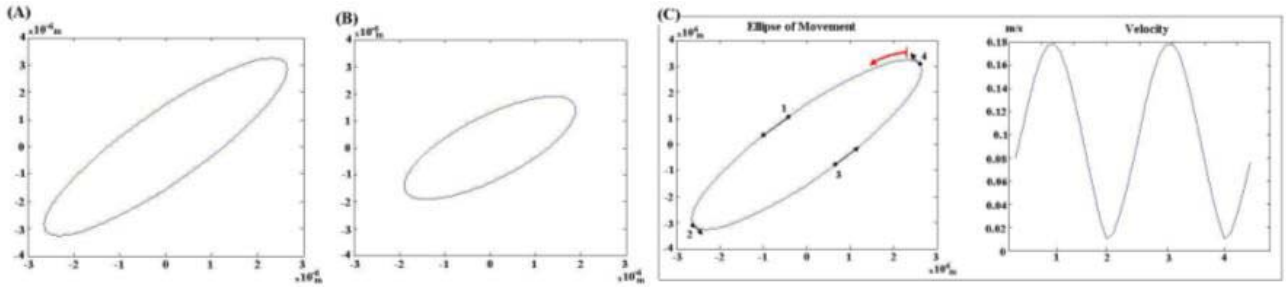

Figure 4. (A) The ellipses of movement without damping and (B) with structural damping; (C) velocities of each point of the ellipse of movement.

As it was expected, the addition of the structural damping in the motor reduces the displacement amplitude together with a change of phase, evidenced by the axis inclination of the ellipse, as it can be seen in the figure above.

Through the calculation of the ellipse of movement considering damping, the velocities of each point of the ellipse can also be calculated, as the Fig. (4c) shows.

Through graph above, in point 1 of the ellipse of movement in Fig.(4c), which is the actual contact point between the stator and the carriage, the velocity of the carriage was obtained by using MATLAB. This velocity is equal to 0.1785 m/s

5.2. Visualization of the displacement and the mechanical stresses during the operation

Continuing with the simulations through ANSYS, a harmonic analysis was performed to obtain Von Mises mechanical stresses during the motor movement considering the application of a sinusoidal wave of electrical voltage of 500V amplitude and 42 kHz frequency in the horizontal ceramic and the same wave with a phase difference of 90º in the vertical ceramic. Using MATLAB, as already mentioned, an animation for the visualization of the mechanical stress during the movement of the motor was developed. This animation can be seen in the site (http://www.geocities.com/piezeletricos)

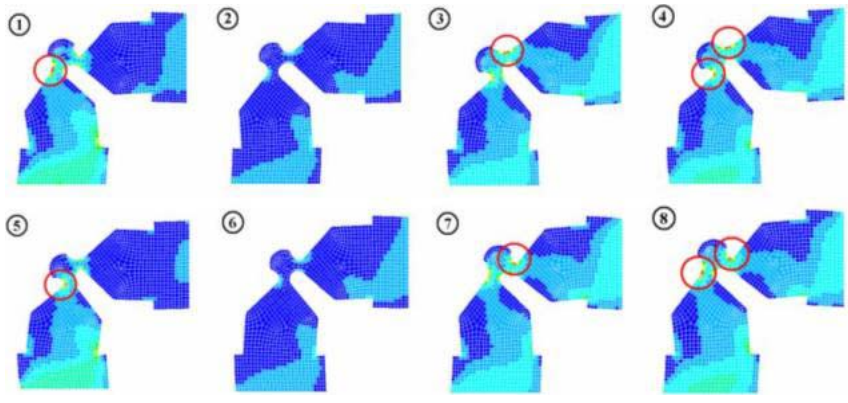

Figure 5. Visualization of the displacement and Von Mises mechanical stresses during the operation.

From the figure above, it can be concluded that the region of constriction (thin part of the structure) has a strong stress concentration (marked with a red circle in some frames above), because it presents the largest Von Mises mechanical stress, 19.2 MPa (calculated by using ANSYS). This can be an important factor for the choice of the type of material to manufacture this structure.

5.3. Propagation of a traveling mechanical stress wave through the motor

To understand better the propagation of a traveling mechanical wave through the motor structure, a transient analysis was performed. In this analysis, only one cycle of a sinusoidal electrical wave was applied to the horizontal ceramic to simulate the behavior of Von Mises mechanical stresses in the structure.

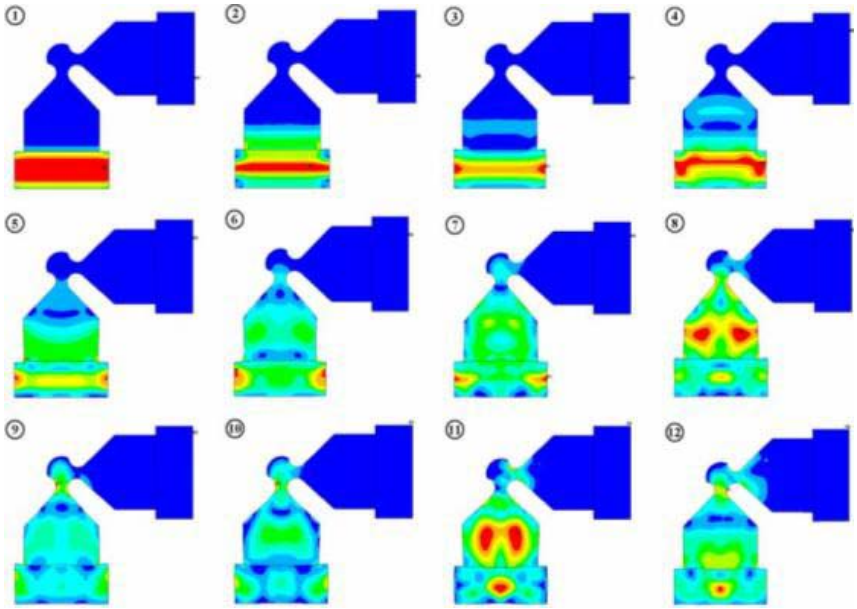

Figure 6. Visualization of Von Mises mechanical stresses during the propagation of a traveling wave.

From this same simulation, the following graph of Von Mises mechanical stress (for each point indicated in the figure bellow) was obtained in ANSYS.

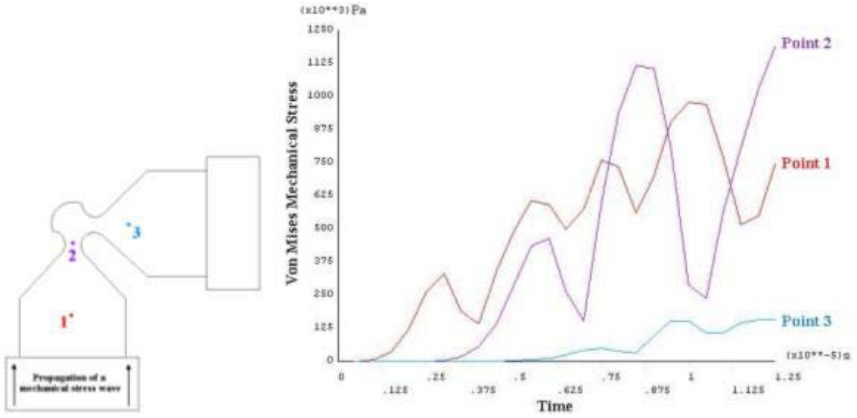

Figure 7. Motor structure (to the left) and graph of Von Mises mechanical stress (to the right).

For this simulation, an animation was also developed. It is available at the site (http://www.geocities.com/piezeletricos).

Figures (6) and (7) indicate that the reflection of the mechanical stress wave in the boundary of the structure raises the value of the mechanical stress. From Fig. (7), it can be concluded that the region which requires the largest mechanical strength is the constriction of the structure, where is located point 2.

5.4. Analysis of optimum frequency of operation

Using the methodology developed in this article, the objective now is to find the motor optimum operational frequency, which means, the frequency that allows the appearance of the larger ellipse of movement. To find this frequency, the motor was simulated in the range of 28 kHz (close to 2nd resonance frequency) to 57 kHz (close to 4th resonance frequency),

because the operational frequency of the motor (42 kHz) is in this range. In the figure below, there are some ellipses of movement (considering the same scale) in the described range above.

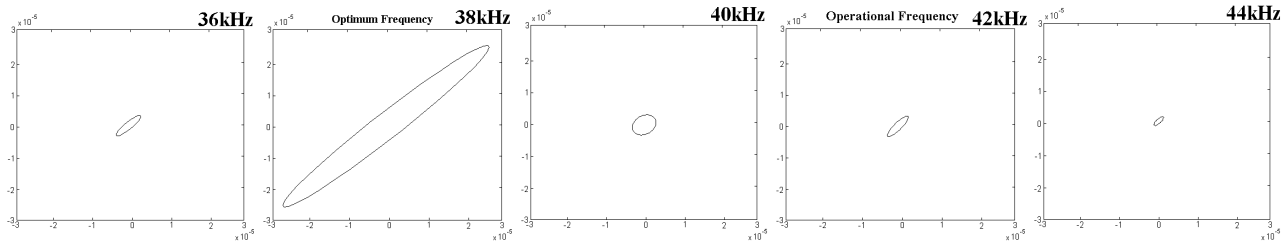

Figure 8. Ellipses of movement of the frequencies of: 36 kHz, 38 kHz, 40 kHz, 42 kHz, 44 kHz.

However, only the movement ellipse is not enough to identify the optimum frequency of operation, also it is necessary the analysis of velocities of these ellipses, which is described in the table below shows for each one of the frequencies above.

Table 1. Values of the velocity for each analyzed frequency.

Frequencies (kHz)	Velocities (m/s)
36	0.1224
38	1.0993
40	0.1292
42	0.1785
44	0.0593

Analyzing Fig. (8), it can be noticed that the frequency which generates the largest ellipse of movement is 38 kHz (for the same analyzed period of time). The same result is shown in Tab. (1), indicating the frequency of 38 kHz as the frequency which generates the largest velocity. These results demonstrate that 38 kHz is the actual optimum frequency of operation of the motor.

Although it is concluded that the optimum frequency of operation is 38 kHz, it must be taken into consideration that the operational frequency of 42 kHz is very close to 38 kHz and is defined for the real motor (see Fig. (2)), which presents a structure with some three-dimensional details (for example, an internal bolt hole).

5.5. Simulation of the motor together with its electrical driving circuit

By simulating the FEM model shown in Fig. (3), using a transient analysis, in which the driving electrical circuit is considered, the following results (graphs (A) and (B)) for the displacement in axes X and Y of the tip of the stator was obtained.

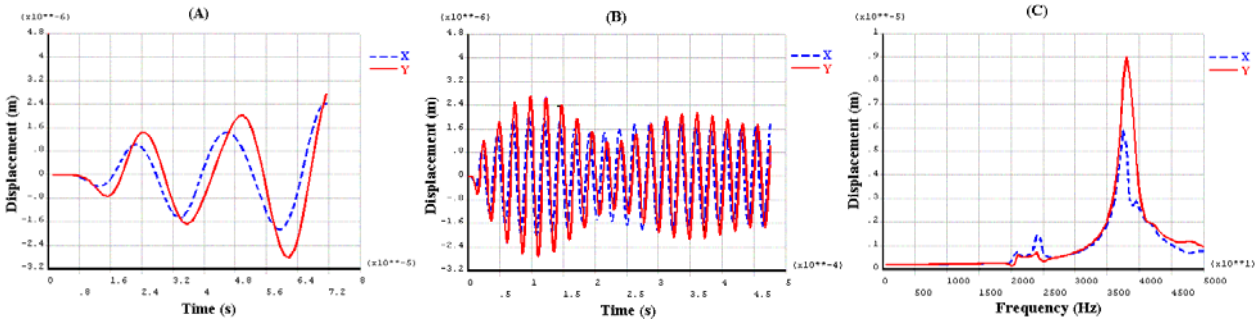

Figure 9. (A) Displacement of the stator tip for 3 periods of the signal; (B) for 20 periods of the signal; (C) displacement of the stator tip in frequency response.

However, as it can be seen in the graph above, the resulted displacement signal in X and Y directions does not stabilize itself for being a transient analysis (see Appendix B).

Therefore, a harmonic analysis was performed. For this one, it was necessary to substitute the electrical source of variable electrical voltage for a source of constant amplitude, as it was already mentioned. The graph (C), in the Fig. (9), for the frequency range from 0 to 50 kHz represent the result of this analysis.

From the graph (C), the effectiveness of the simulation of the motor together with its electrical driving circuit can be proved, because the peaks of amplitude of the displacements in axes X and Y are observed, at about 38 kHz, which is accurately the optimum frequency of operation found in the previous section of this article.

6. Conclusions and Future work

In this work, a methodology for simulating linear piezoelectric motors using FEM in the software ANSYS, together with the software MATLAB was developed.

It was proved the effectiveness of simulating piezoelectric motors together with its electrical driving circuits, which can provide us a better understanding about the motor operation.

As a future work, prototypes of the motor in study will be built with order of magnitude of millimeters. In addition, it will be studied and simulated the contact between the stator and the carriage using software ANSYS.

7. Acknowledgments

The first author is thankful for the support of the FAPESP – Fundação de Amparo à Pesquisa do Estado de São Paulo - through an undergraduate fellowship for the development of this work.

8. References

Frank, J., Koopmann, G.H., Chen, W., Lesieutre, G.A., 1999 "Design and Performance of a High Force Piezoelectric Inchworm Motor", Center for Acoustics and Vibration, Penn State University, *6th SPIE (Annual International Symposium on Smart Structures and Materials)*, Newport Beach, California.

Kagawa, Y., Tsuchiya, T., Kataoka, T., Yamabuchi, T., Furukawa, T., 1996, "Finite Element Simulation of Dynamic Responses of Piezoelectric Actuators", Journal of Soud and Vibration, 191(4), pp. 519-538.

Kurosawa, M.K., Kodaira, O., Tsuchitoi, Y., Higuchi, T., 1998, "Transducer for High Speed and Large Thrust Ultrasonic Linear Motor Using Two Sandwich-Type Vibrators", *IEEE Transactions on Ultrasonics, Ferroelectrics, and Frequency Control*, Vol.15, n.5, p.1188-1195.

Lerch, R., 1990 "Simulation of Piezoelectric Devices by Two- and Three-Dimensional Finite Elements", IEEE, Transactions on Ultrasonics Ferroelectric and Frequency Control, Vol.37, nº 2, pp. 237-246.

Moaveni, S., 1999, "Finite Element Analysis – Theory and Application with ANSYS", Prentice Hall, New Jersey.

Ostergaard, D.F., Pawlak, T.P., 1986, "Three-Dimensional Finite Element for Analyzing Piezoelectric Structures", Swanson Analysis System, Inc., IEEE, Ultrasonics Symposium, Houston, EUA, pp. 639 – 644.

Roberts, D., 1999, "Development of a Linear Piezoelectric Motor based upon the Inchworm Model", Mechanical Sciences Sector, Dera, Farnborough, Hants, *6th SPIE (Annual International Symposium on Smart Structures and Materials)*, Newport Beach, California.

Sashida, T., Kenjo, T., 1993 "An Introduction to Ultrasonic Motors", Clarendon Press – Oxford.

Wang, J. S., Ostergaard, D. F., 1999 "A Finite Element-Electric Circuit Coupled Simulation Method for Piezoelectric Transducer", ANSYS, Inc., 1999 IEEE Ultrasonics Symposium, pp. 1105-1108.

Simulation of a Linear Piezoelectric Motor by Using Finite Element Method Web Site

9. Appendix

A. Properties of materials considered in the FEM model

The properties of the aluminum structure of the stator and of simulated piezoelectric ceramics considered in this article are equal to the following:

Aluminum Structure:
Density $\rho = 2800$ kg/m^3
Young Modulus = $7.1.10^4$ MPa
Poisson Coefficient $\upsilon = 0.33$
Damping Coefficient $\beta=4.10^{-7}$

Piezoceramics:
Density $\rho = 7800$ kg/m^3
Damping Coefficient $\beta=5.10^{-8}$
Permittivity: $\varepsilon_x = 8.1066.10^{-9}$ F/m
$\varepsilon_y = 7.3455.10^{-9}$ F/m
$\varepsilon_z = 8.1066.10^{-9}$ F/m

Mechanical stiffness matrix:

$$[c] = \begin{bmatrix} 12.1 & 7.52 & 7.54 & 0 & 0 & 0 \\ 7.52 & 11.1 & 7.52 & 0 & 0 & 0 \\ 7.54 & 7.52 & 12.1 & 0 & 0 & 0 \\ 0 & 0 & 0 & 2.11 & 0 & 0 \\ 0 & 0 & 0 & 0 & 2.11 & 0 \\ 0 & 0 & 0 & 0 & 0 & 2.28 \end{bmatrix} 10^{10}\text{N/m}^2$$

Piezoelectric matrix:

$$[e]^T = \begin{bmatrix} 0 & -5.4 & 0 \\ 0 & 15.8 & 0 \\ 0 & -5.4 & 0 \\ 12.3 & 0 & 0 \\ 0 & 0 & 12.3 \\ 0 & 0 & 0 \end{bmatrix} \text{C/V}$$

B. Discussions about the simulation of the movement of the motor in transient analysis

For the visualization of displacement and mechanical stresses during the movement of the motor, a transient analysis would supply the images of the visualization each instant of analysis time, not being necessary to perform a harmonic analysis or use MATLAB to rebuild the finite element structure. However, the resulting signal did not stabilize itself in 20 periods of input signal, indicating a beating in the signal. To analyze this beating, the frequency spectrum of this 20-period sinusoidal signal of 42 kHz, using 400 points of discretization (20 points per period) is shown in the Fig.(10a), obtained using the Discrete Fourier Transform function of MATLAB.

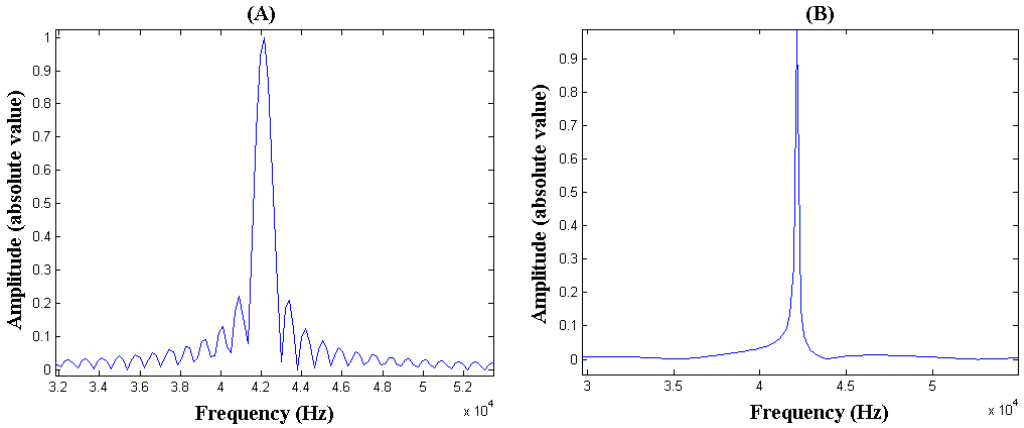

Figure 10. Frequency Spectrum of the signal with (A) 20 periods and (B) 200 periods

In the figure above, observe that there are many components of frequency in the signal, which probably is the cause of the beating observed, once some of these components of frequency coincide with motor resonance frequencies. To solve this problem, it is necessary to increase the number of periods of the input signal (increasing, consequently, the signal discretization). After an iterative process, it was concluded that a signal with 200 periods (see the Fig. (9)) would practically eliminate these frequency components.

Considering a discretization of 20 points per period (not to harm the sampling of the input signal), 200 periods generate 4000 points of input signal. However, ANSYS has a limit of 1000 points. For this reason, the transient analysis is impracticable to allow visualization of the displacement and the mechanical stresses during the motor movement and, therefore, the harmonic analysis must be used.